Prediction of Base Pressure in a Suddenly Expanded Flow Process at Supersonic Mach Number Regimes using ANN and CFD

J. D. Quadros[1] and S. A. Khan[2]

[1]*Department of Mechanical Engineering, Birla Institute of Technology, Off-shore campus, Ras Al Khaimah, UAE*
[2]*Department of Mechanical Engineering, International Islamic University Malaysia, Kuala Lampur, Malaysia*

†*Corresponding Author Email: qjaimon@yahoo.co.in*

ABSTRACT

Sudden expansion of flow in supersonic flow regime has gained relevance in the recent pasts for a wide run of applications. A number of kinematic as well as geometric parameters have been significantly found to impact the base pressure created within the suddenly expanded stream. The current research intends to create a predictive model for base pressure that is established in the abruptly extended stream. The artificial neural network (ANN) approach is being utilized for this purpose. The database utilized for training the network was assembled utilizing computational fluid dynamics (CFD). This was done by the design of experiments based L_{27} Orthogonal array. The three input parameters were Mach number (M), nozzle pressure ratio (NPR) and area ratio (AR) and base pressure was the output parameter. The CFD numerical demonstrate was approved by an experimental test rig that developed results for base pressure, and used a nozzle and sudden extended axis-symmetric duct to do so. The ANN architecture comprised of three layers with eight neurons in the hidden layer. The algorithm for optimization was Levenberg-Marquardt. The ANN was able to successfully predict the base pressure with a regression coefficient R^2 of less than 0.99 and RMSE=0.0032. The importance of input parameters influencing base pressure was estimated by using the ANN weight coefficients. Mach number obtained a relative importance of 47.16% claiming to be the most dominating factor.

Keywords: Base pressure, Mach number, Artificial Neural Network (ANN), Computational Fluid Dynamics (CFD).

NOMENCLATURE

A	exit area of the nozzle	W	weight
A^*	Throat area of the nozzle	y	axial distance
b	bias		
C_p	specific heat of air Constant pressure	**Subscripts**	
g	linear function	AR	Area Ratio
I	Relative importance	ANN	Artificial Neural Network
M	Mach number at the nozzle exit	ART	Adaptive Response Theory
P	static pressure	CFD	Computational Fluid Dynamics
P_0	stagnation pressure	NPR	Nozzle Pressure Ratio
P_b	base pressure	m	mainstream or number of neurons in hidden layer
P_a	ambient pressure		
Q	number of data points	min	minimum
q	index of data	max	maximum
S	slope	s	number of neurons in hidden layer
U	input data	h	number of neurons in input layer

1. INTRODUCTION

In view of aerodynamic optimal design, an critical area of advancement in the recent years has been base pressure at higher Reynolds number. The base drag that originates at the blunt base of a projectile and missile may be considered as a significant fraction of the total drag. For instance, base drag could possibly be about 50 percent of the total drag for an off powered missile i.e. (lack of jet flow at the base) (Bansal and Sharma, 2018). This has resulted in its wide applicability and hence extensive studies have been conducted on base pressure with fundamental insistence provided to either increase or decrease of base pressure and its control. Suddenly expanded flows generally employ an internal flow apparatus as it has a number of advantages over traditional unconfined viz. (wind tunnel) test procedures. The internal flow apparatus eliminates the use of tunnels with which, one would be able to reduce the size of the air supply required and this would eventually lead to minimum interference at the wall that would disturb the flow. Additionally, stings (test fixture on which models are mounted for testing) and various other backup mechanisms are also avoided. The most decisive advantage of using an internal flow apparatus is sophisticated static pressure and surface temperature measurements could be made along the duct entrance as well at the expansion section (Karthick *et al.,* 2018). These measurements are distinctly worthwhile for testing theoretical predictions adequately. Therefore when we compare wind tunnel tests and internal flow apparatus, the results obtained more or less would be the similar. However, an additional error would be associated with wind tunnel tests due to installation of support mechanism and stings and hence avoided.

Quite a few researchers have developed numerous techniques to control base pressure by means of active and passive controllers (Alvi *et al.,* 2003). Active control by blowingithrough orifices has been found to be quite influential in varying theibase pressure (Baig *et al.,* 2011). Works contemporary to the present study have been reviewed in the section below. As of for now, no work as yet has come to the notice of authors that reports modeling of base pressure using ANN and CFD. A typical flow that is suddenly expanded is described byfflow separation, flow recirculation andjreattachment (Khan and Rathakrishnan, 2006). The suddenly expanded flow process has beenfshown in Fig. 1. It must be notified that, quite a few experiments that have been conducted on expanded flows by considering various geometric and kinematic factors. However this has implied enormous economical andfcomputational cost. Such costs can easily be reduced by use of surrogate methods viz. ANN and CFD for obtaining important correlations for prediciting base pressure. Considerable amount of literature is available on the sudden expansion problem. Apparently, the problems have considered geometric and flow parameters. The sudden expansion problem was first investigated by Korst (1956) wherein the flow downstream the base was supersonic in nature. It was observed that, there was interaction amidst the free and the shear stream and a physical model was developed to understand this. Khan and Rathakrishnan (2002) conducted experiments to understand micro jet effects on base pressure behavior for a nozzle that was over expanded. The study showed that base pressure could be easily regulated by actively controlling the jets. Khan and Rathakrishnan (2003) conducted trials for manipulating base pressure. The control parameters used were Mach numbers (M) (1.87, 2.2 and 2.58) and NPRs (3, 5, 7, 9 and 11). The trials showed base pressure manipulation to a level of 95 percent. Khan and Rathakrishnan (2004a) conducted studies to see if base pressure could be controlled at an under expansion level for nozzles of Mach 1.25, 1.3, 1.48, 1.6, 1.8 and 2.0. The study corroborated that micro jets are competent active regulators and can control base pressure to a considerable extent. Khan and Rathakrishnan (2004b) conducted flow expansion studies for nozzles of M= 1.25, 1.3, 1.48, 1.6, 1.8 and 2.0 undergoing correct expansion. However for this particular case the micro jets hardly influenced base pressure. This was due to a weak wave that occurred at the nozzle exit/duct interface. Rathakrishnan and Sreekanth (1984) through experiments opined that flow and geometric control parameters viz. AR (area ratio), NPR (nozzle pressure ratio) and L/D (length to diameter ratio) vastly influenced base pressure and also that for a particular L/D the pressure at the maximum level can be determined if the AR and NPR are known. Quadros *et al.* (2016) used the DOE approach and predicted base pressure by use of an L_9 Orthogonal array. M, L/D and AR were the control parameters. Multiple linear regression models were developed for base pressure and furthermore analysis of variance was conducted. The regression models developed were able to predict base pressure successfully with accurate predictions. Quadros *et al.* (2018) developed non-linear regression models by using central composite design (CCD) and Box Behnken design (BBD) to predict base pressure for different parameters. Fifteen test cases were performed in order to check the validity of the models developed. BBD was found to be the model that predicted accurate base pressure when compared to the CCD models. Although the experiments have proven that base pressure is greatly affected by different parameters, no predictive approach using CFD/ANN has been proposed as yet. Therefore it is largely essential that a predictive tool be developed to know beforehand the base pressure as it will be of enormous assistance for various space programs for understanding base pressure behavior fully. In this paper, artificial neural network (ANN) approach has been utilized to predict base pressure. A DOE based L_{27} orthogonal array has been used to train the ANN network using the results from computational fluid dynamics. Additionally, a sensitive study has also been undertaken to define the relative importance of input variables.
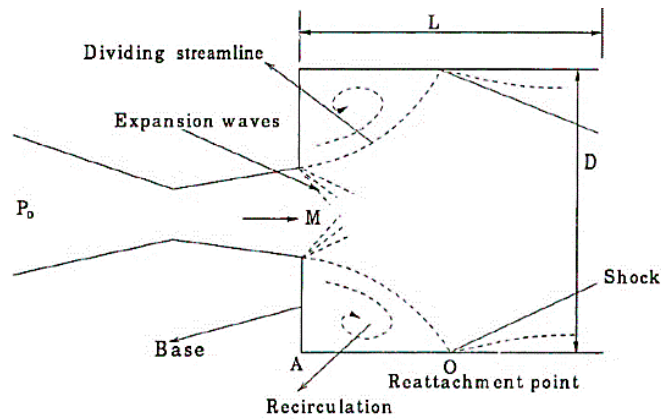
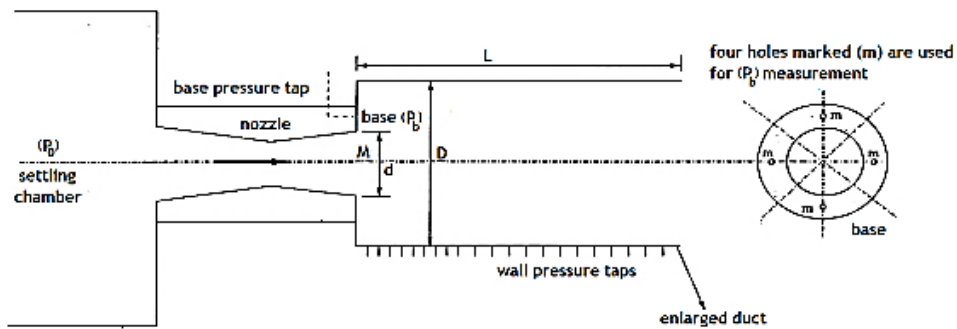**Fig. 1. Suddenly expanded flow process.**

Fig. 2. Experimental set up.



Fig. 3. Convergent divergent nozzle.

Fig. 4. Suddenly expanded ducts.

2. EXPERIMENTAL PROCEDURE

Figure 2 shows the experimental set up for the present study (Quadros *et al.,* 2016, 2018). The set up consists of a compressor, settling chamber, nozzle containing four holes at its exit periphery that are used to measure base pressure (P_b) and a suddenly expanded duct. Apparently, air is maintained at a high pressure in the compressor. The air which is compressed is then passed onto the settling chamber where it is regulated to the desired degree. The air from the chamber is then passed into the expanded duct through the nozzle. As the movement takes place at the nozzle exit periphery, measurement of base pressure is taken through the pressure taps. The control parameters for conducting the experiments were Mach numbers (M) maintained at 2.0, 2.5 and 3.0, nozzle pressure ration (NPR) maintained are 5, 7, and 9, and area ratio (AR) were 3.24, 4.84 and 6.25 respectively. The L/D for the study was maintained constant at 5.

Nozzles shown in Fig. 3 of convergent-divergent (C-D) sections possessing a common exit diameter of 10mm that correspond to Mach numbers 2.0, 2.5 and 3.0 were fabricated as per (Quadros *et al.,* 2018). The ducts appeared in Fig. 4 were fabricated of brass and had diameters of 18mm, 22mm and 25mm inferable from ARs of 3.25, 4.75 and 6.25
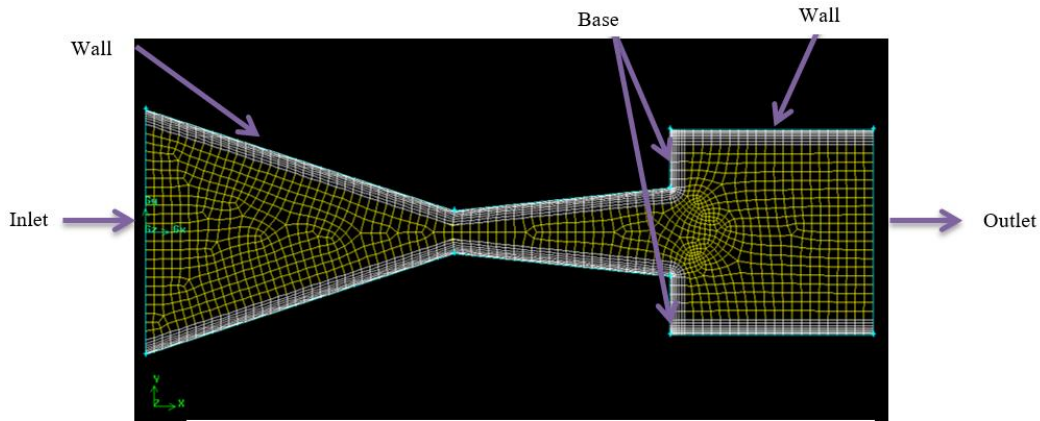
**Fig. 5. Meshed model of the nozzle and the expanded duct**.

respectively. The estimations of base pressure were done without the utilization of microjets. Since the stream field is very reactive to the duct surface, it was made sure that the abruptly extended ducts were given a prudent surface completion in order to accomplish precise base pressure results. A PSI framework 2000 pressure transducer was employed for evaluating base pressure. This transducer had 16 channels with a showcase of pressure going from 0-300 psi. The information was shown at an averaged value of 250 samples for each second. All the non-dimensional base pressure shown were inside a vulnerability band of ±2.6 percent. Every one of the outcomes is repeatable inside ±3 percent.

3. COMPUTATIONAL METHOD

Various engineering fields viz. aerodynamics, thermal engineering use numerical analytical techniques (Tu *et al.,* 2007). The evolution of codes and computers has made it easier to solve problems related to fluid flow due to availability of governing equations in partial derivative and integral form. The use of numerical techniques in studies pertaining to nozzle flow is already conducted at the international level by a number of researchers. However studies with respect to flow behaviour post expansion situated downstream of the nozzle has rarely been done.

GAMBIT 16 software of commercial license has been used to create the nozzle geometry and duct geometry. This software uses the base, vertex and edge command to construct the nozzle and duct geometries as required as per the dimensions. Post completion of the geometry, the nozzle and duct are meshed over their faces and edges. A technique called as multi block was used to generate a structured mesh possessing quadrilateral cells. The mesh is presented in Fig. 5. The mesh size consisted of 3,836,644 cells, based on a mesh independence study with a y+ between 0.1 and 1. Meshes with 3,836,644 and 4,890,868 cells depicted an average difference in base pressure of 0.37, and because of this, a mesh with 3,836,644 cells was preferred as it

incurred lesser computational cost (Fig. 6). After meshing the model, it was imported to the ANSYS Fluent software in order to carry out base pressure simulations. The boundary growth ratio was used in two volume grid regions i.e. air flow evaluation at the base region is carried out by analytical method. This is generally done for simple laminar flows. The cases where flow process experiences turbulence tends to develop ambiguity for solving Navier-stokes and continuity equation. In order to overcome this problem, time averaged Navier-stokes equation is used alongside turbulent models. The wall treatment is done by selecting the viscous k-ε model (Launder and Spalding, 1972). The k-ε model is robust and has a feasible computation time and widely used for simulation in auto industries. Due to nature of flow which is supersonic, a density based solver is used. A time step of 0.000143 seconds has been utilized on the basis of Courant number (CN)<1. This number gives out data relevant to fluid movement through computational cells. When the CN is less than 1, the fluid particles move through cells taking one step at a time. Similarly CN > 1 enables fluid particle movement through multiple cells at each time steps.
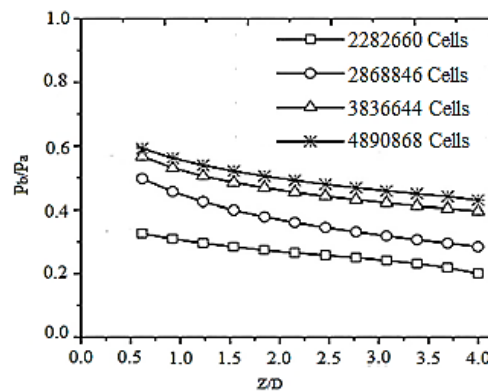
Fig. 6. Cells for meshing.

The criterion for convergence of continuity is fixed to 10^{-4}, and the criterion for energy convergence is fixed to 10^{-6}. Due to the turbulence of the flow,

unsteady time accurate simulations were performed. A second order upwind scheme is implemented by solving partial differential equations in order to obtain accuracy in base pressure results. The boundary conditions are: Inlet condition: operating pressure at the nozzle inlet where stagnation pressure (P_0) is applied; ii) Outlet condition: Base pressure measured at the point where exit periphery of the nozzle and expanded duct intersect each other. The computations were carried out using an Intel core i7-5775C desktop processor.

3.1 ANN Model for Predicting Base Pressure

Artificial neural network (ANN) (Baymani *et al.,* 2015) is a paradigm that processes data actuated by nervous systems viz. brain, process certainties. It is formed out of a huge number of neurons that are interconnected and working single handedly to handle conflicting issues. The cases undertaken in ANN include the ones that conform to synaptic unions prevailing amidst the neurons. A few applications for ANN have been found in the field of fluid mechanics as well. Problems involving non-linearity have found ANN beneficiary for its modeling (Gholami *et al.,* 2015). Furthermore, ART2 i.e. (Adaptive Resonance Theory) based ANN has proved that it can accurately predict velocities pertaining to fluid flow upto the range of 96.4% (Fontama *et al.,* 1997). Various friction factors for water flow in tubes possessing internal fins are being successfully predicted by using the ANN technique. The ANN results were found to be satisfactory (Gregory *et al.,* 2007). Therefore the present study also aims to employ the ANN technique to model the flow process that is expanded suddenly established by parameters viz. M, NPR and AR. The data procured via CFD modeling for base pressure was used to train, test and validate using the neural network model equipped in MATLAB 7.6.0 (R2014a). The study implemented a network that comprised of three layers namely input, hidden and output layer. The number of parameters in the study regulated the number of neurons in the various layers. In a view of achieving ultimate output efficiency, optimization of the neurons in the hidden layer was done. The number of input classifications and the input vector size generally determine the hidden layer neurons. The presence of too many neurons may result in an over fit whereas a few neurons may under fit. In the hidden layer, each neuron has been assigned a bias b_i. This bias is used to define the hidden neuron input by getting added to the summation of weighted input. An example for this is Eq. (1)

$$n_1 = W_{1,1}In_1 + W_{1,2}In_2 + .. + W_{1,k}In_k + b_1 \qquad (1)$$

The output layer calculates the weighted sum of hidden layer signals and two new co-efficients are generated i.e. W_0 and b_2 that correlate the hidden neuron layer weight to the output neuron layer weight. Then the network output can be calculated by Eq. 2.

$$y = g[W_0 f (W_i In + b_1) + b_2] \qquad (2)$$

The primary step in the ANN methodology is delineating the algorithm that is used to train the net. This algorithm basically modifies the biases and weights in a view to attain minimal error function amid network predicted output and the database stored output (Fig. 7). Known for its reliability and rapid convergence, Liebenberg-Marquardt algorithm was used for training the network. The evaluation of the ANN performance was done by root mean square error (RMSE) and the regression co-efficient measured by Eqs. (3) and (4). A critical factor that effects ANN prediction is data population. It is imperative that data population avoids repetitive data. The present work conducts the training of the data population based on CFD computations. The CFD computations however are quite time consuming and aren't feasible for a large database. Therefore design of experiments based orthogonal arrays viz. L_9, L_{27} could be used to construct a valid database. With these levels, each parameter can use levels that represent superior and inferior limits within a visible range. The numbers of samples are characterized by 3^n, where 3 describe three levels and n is the variable count.
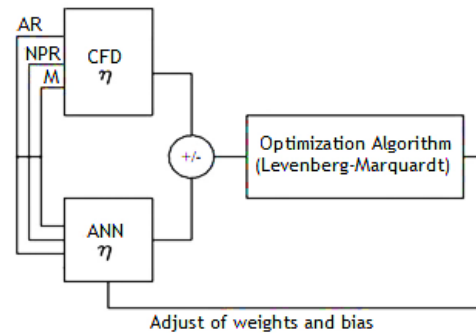

Fig. 7. Levenberg-Marquardt optimization algorithm.

An algorithm was used for geometry construction for the CFD code to run in an automated manner. The algorithm forms the matrix set up by L_{27} orthogonal arrays. This array consisted of 27 (samples) rows and 3 (parameters) columns. Table 1 represents the values of the matrix. Out of the 27 samples, 18 samples of the dataset were used for normalization, 9 were used for both training and testing. All data is normalized in a range of 0.1–9 using Eq. (4). Here u_i is the normalized value, U_i is the value of data prior to normalization and u_{min} and u_{max} are data's in the superior and inferior range respectively. The variation of hidden layer neurons leads to achieving optimal accuracy. The current study found 6 neurons to be convenient and the training for ANN is as shown in Fig. 8. The learning rate was initially set to 0.9 for faster training of the network. But since the error was high and in order to avoid the stalling of training process, the learning rate was decreased by a factor of 0.1. Subsequently, a progressive decrease in the learning rate was delivered as per the diminution in the training error. Prolonged training can lead to ANN recollecting input output pattern, leading to the outcome of rational capacity. For this

particular reason, the present study implemented 18 data points that were normalized for training with approximately 2000 iterations. Apparently, 250 iterations found that there was an error increase for checking dataset. Hence, 250 iterations were predicted to be favorable for the present network simulation. Table 2 shows data set to train the ANN. This table comprises of details pertaining to the input parameters and results of experimental and CFD base pressure.

$$RMSE = \sqrt{\frac{\sum\limits_{q=1}^{Q} (\eta_{ANN} - \eta_{CFD})^2}{Q}} \qquad (3)$$

$$R^2 = 1 - \frac{\sum\limits_{q=1}^{Q} (\eta_{q,ANN} - \eta_{q,CFD})^2}{\sum\limits_{q=1}^{Q} (\eta_{q,CFD} - \eta_m)^2} \qquad (4)$$

$$u_i = 0.8 \frac{[U_i - U_{min}]}{[U_{max} - U_{min}]} \qquad (5)$$

Table 1 Parameters and their levels

Levels	M	NPR	AR
1	2.0	5	3.24
2	2.5	7	4.84
3	3.0	9	6.25

4. RESULTS AND DISCUSSIONS

4.1 CFD Results

The base pressure results for CFD and their comparison with the experimental base pressure have been presented in Fig. 9. These results are for various NPR's and a constant L/D of 5. The results for base pressure obtained are non dimensionalized by divining them by ambient atmospheric pressure i.e. $(1.013 \times 10^5$ Pa$)$. The CFD results are found to be in good agreement with the experimental results. Further sections below give a detailed examination of analytical and experimental results. The maximum error is observed for the test cases in the L_{27} array and is presented.

It is clearly shown that base pressure increased with Mach number increase and simultaneously decreases when NPR is increased from 5-7 and thereafter from 7-9. The physical purpose behind this conduct is that the flow stays over extended for this scope of the expansion level (Khan and Rathakrishnan, 2006). This is because of high over development of the flow at higher Mach quantities of 2.5 and 3.0 where a more grounded impact at the nozzle exit is observed. Anyway these shocks have bigger shock edges and consequently stream deflections are little. Accordingly these shocks won't direct base pressure

in the base area as this area is commanded by recycling stream instead of shock stream, in this manner increasing base pressure (Quadros *et al.,* 2016).

Table 2 Experimental parameters and the values of non- dimensional base pressure

M	NPR	AR	Exp (Pb/Pa)	CFD (Pb/Pa)
Training data set				
2.0	5	3.24	0.126	0.12
2.0	7	4.84	0.174	0.18
2.0	9	6.25	0.155	0.15
2.5	5	3.24	0.476	0.52
2.5	7	4.84	0.489	0.51
2.5	9	6.25	0.518	0.56
3.0	5	4.84	0.763	0.78
3.0	7	6.25	0.737	0.71
3.0	9	3.24	0.469	0.45
2.0	5	6.25	0.553	0.59
2.0	7	3.24	0.119	0.10
2.0	9	4.84	0.111	0.11
2.5	5	4.84	0.596	0.62
2.5	7	6.25	0.556	0.61
2.5	9	3.24	0.049	0.05
3.0	5	6.25	0.814	0.87
3.0	7	3.24	0.595	0.58
3.0	9	4.84	0.469	0.46
Testing data set				
2.0	9	3.24	0.165	0.15
2.0	5	4.84	0.479	0.51
2.5	7	3.24	0.347	0.31
2.0	7	6.25	0.327	0.30
3.0	5	3.24	0.695	0.71
2.5	5	6.25	0.679	0.69
Checking data set				
3.0	9	6.25	0.651	0.67
2.5	9	4.84	0.431	0.43
3.0	7	4.84	0.699	0.72
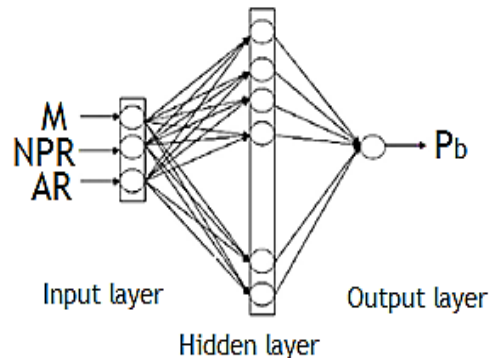
Fig. 8. Neural network architecture.

For a specific Mach number, the NPR deals with the dimension of advancement of base pressure. A closer and authentic view at the stream process at
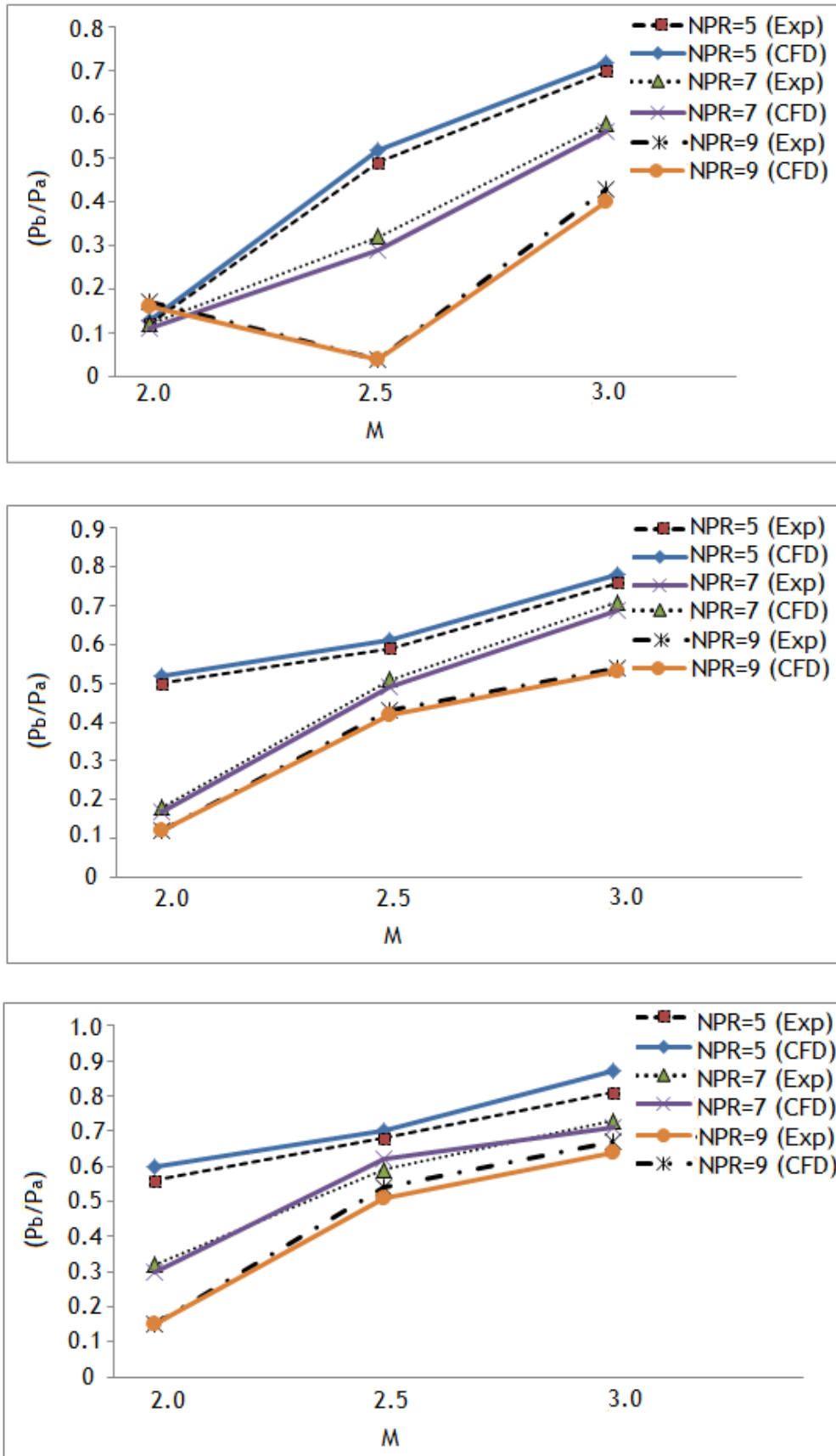
Fig. 9. Variation of non- dimensionalized base pressure with respect to Mach number for various NPRs.

the base of the conduit would possibly give an explanation to this lead. For the most part, the base pressure is a consequence of the advancement level that occurs at the nozzle exit. As the NPR builds the level of over-development descends, thus the angled shock at the nozzle exit becomes anemic than those for lower NPRs. This curtails the swinging away motion of the approaching flows thereby leaving the vortex untouched. The nozzle lip will always tend to have an inflated fan and an angled shock for over and under expanded stream flows (Farahani *et al.,* 2017). Apparently for most cases, the flow from a C-D nozzle will either be correctly, under or over expanded. These are appeared in Figs. 10(a, b and c) individually. Moreover, for a converging nozzle, flow will always be correctly expanded and also the base pressure is equal to the pressure at the nozzle exit. In this study, we are discussing the flow at Mach 2.0. 2.5 and 3.0. Generally for correct expansion the NPR required would be 7.8, 17 and 37. This requirement of NPR is quite high, hence the experiments were carried out for over, correct and under Mach 2.0. However for Mach 2.5 and 3.0 the nozzles were tested for over expanded case only. For a fixed area ratio and diverse Mach numbers, the magnitude of reattachment remains constant. The reattachment magnitude and base pressure is firmly altered by NPR which also precepts the expansion level (Khan and Rathakrishnan, 2002). The L/D ratio is a critical parameter that governs the reattachment magnitude. At this point, back pressure impacts the NPR flow field in the duct. A minimal duct length is always required for the flow to reattach. The literature reports that an L/D of 5 is required for flow to reattach to the duct walls post its separation (Quadros *et al.,* 2017). Thus from the present study, it can be concluded with evidence that, the experimental and CFD results are well in match with each other for distinguished parameters viz. M, NPR and L/D. The area ratio also plays an important role in controlling base pressure. These values are found to be high for high area ratios and are shown in Fig. 9(c). for all the NPRs of the current study. Our study has area ratios fixed at 3.25, 4.84 and 6.25 for each of the experimental case. With respect to these aspect ratios, any change in M and NPR would lead to a considerable change in base pressure. This base pressure hike is due to the layer which shears at the nozzle exit and takes a bit of additional time to re attach resulting in higher base suction (Khan and Rathakrishnan, 2004b).

CFD computations have been performed for a few training data sets as shown earlier in Table 2. Figure 11(a) shows the non-dimensional pressure results for M=3.0, NPR=7, and AR=6.25. For comparison with the experimental value, this value is non-dimensionalized by dividing it by the atmospheric pressure value i.e. (P_a=1.013×10^5 Pa). The pressure at the base region i.e. base pressure is found to be 0.71, which is in very good agreement with the corresponding experimental value of 0.737 (Table 2). Similarly Fig. 11(b) shows a non- dimensional base pressure of 0.56 and its corresponding experimental value is 0.518. Figure 11(c) showed a non-dimensional base pressure of 0.87 with its corresponding experimental value being 0.814. On

this account, each of the CFD obtained value was subjected to comparison with experimental base pressure. Thus the CFD results obtained have been matched quite well with the experimental ones (Table 2). For all the cases compared, a maximum deviation of 11.51% was observed. Therefore the CFD tool was found to be satisfactory in predicting base pressure. The percentage error testifies the ability of the proposed model approaching the experimental outcomes.

(a)

(b)

(c)
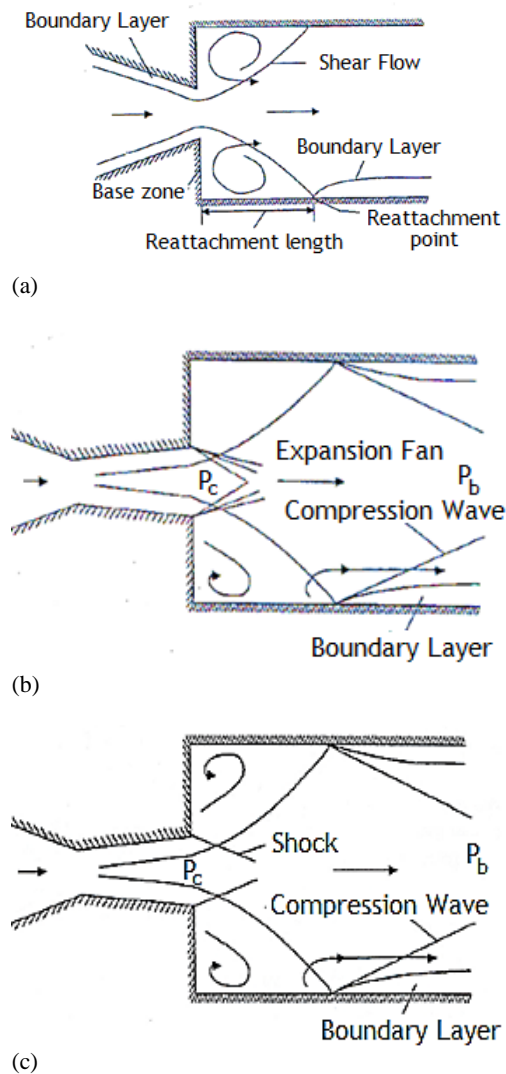
Fig. 10. Flow fields for a) over expansion; b) under expansion and c) correct expansion (Wilcox, 1988).

The CFD results in horizontal plane view show a sizable zone of rotating air mass i.e. recirculation zone at the nozzle exit/duct interface. Due to the existence of this zone at the expanding channel, a considerable amount of non-uniformity is inducted in the flow. This rotating mass prevents the flow coming from the upstream thereby compelling the flow to change its direction towards the alternate side of the duct. This leads to the formation of flow separation. The intensity of the recirculation zone is

(a)

(b)

(c)
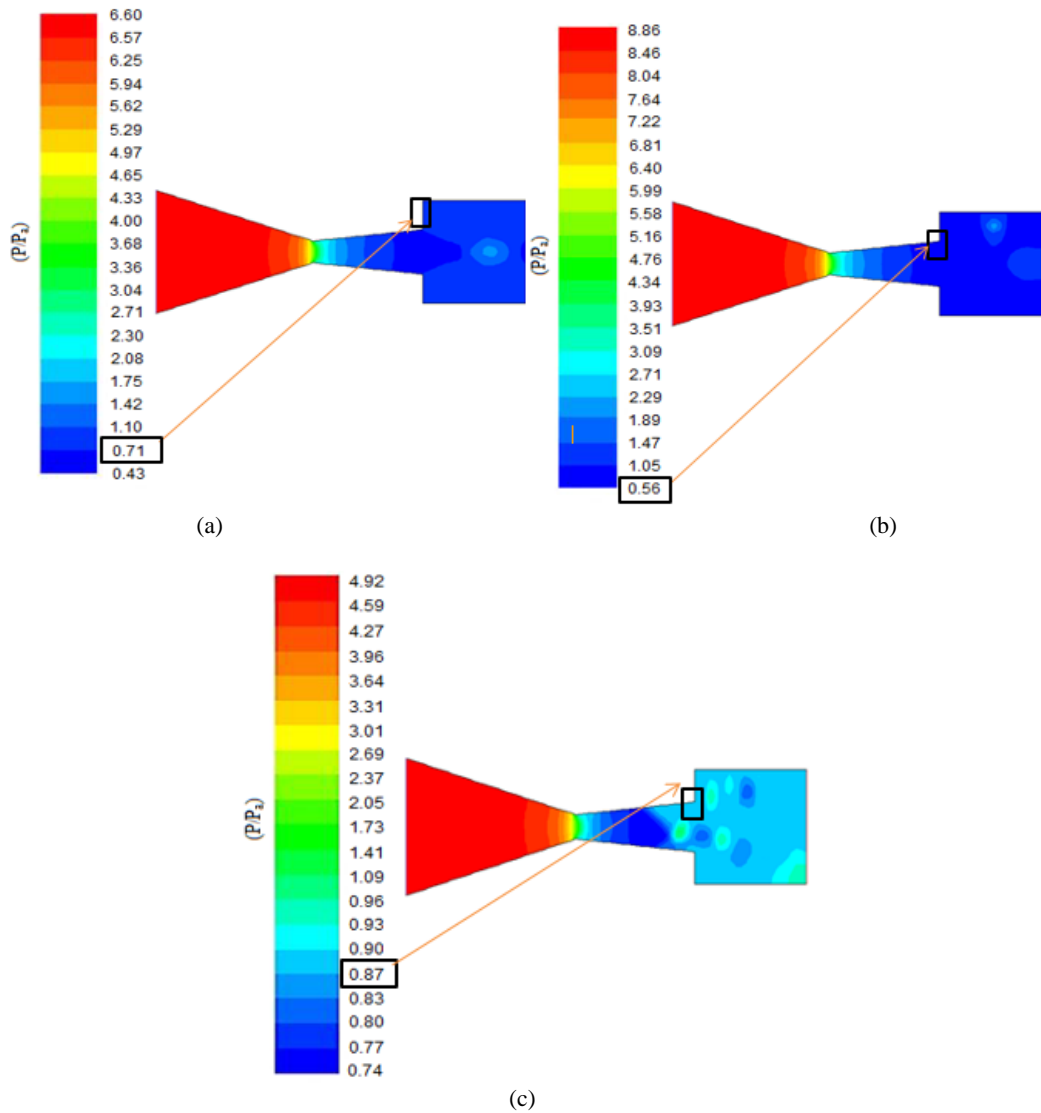
Fig. 11. CFD results for test case a) M=3.0, NPR=7, and AR=6.25; b) M=2.5, NPR=9, AR=6.25 and c) M= 3.0, NPR=5, and AR=6.25.

maximum at the plane passing through the entrance of the duct, where the circulation reaches its ultimate velocity and curtails steadily at the duct surface (Montazer *et al.,* 2018). This is why a sense of non-uniformity will always be associated with recirculation zones (Fig. 11 b & c). At this moment, the base region experiences the flow being turned away due to the occurrence of shock at the nozzle exit. This undermines the vortex strength that is located at the base (Khan and Rathakrishnan 2004a). This eventually causes a slight decrease in base pressure. This problem can anyway be solved by harboring micro jets. These jets would be able to infuse mass through a chamber without causing any disturbance in the base pressure (Khan and Rathakrishnan, 2004b). Thus from the results above, one will be able to clearly understand the extent of manipulation to be made to parameters such as Mach number and area ratio in order to control base pressure owing to its increase or decrease. Therefore it can thoroughly concluded that the size and position of the recirculation zone could be easily predicted by

numerical computation. The above profiles in the expansion region show a few disturbing zones which are basically created due to the recirculation zone. The formed vortex zone tends to advance due to interference and one more is created as a result of return flow.

4.2 Model Developments and Results

The normalized range of 0-1 has been used for input/output variables and has implemented for the present study. A standardized logistic sigmoid function was used in the hidden and output layers. 250 iterations have been used to train the ANN. The training objective was employed for the first 18 data sets. The value of base pressure predicted by ANN was subjected to comparison with its corresponding CFD value. The linear regression results for training and validation has been shown in Fig. 12. The linear regression coefficient was R^2 = 0.99712 and RMSE was 0.0032, which

Table 3 Coefficients of weights and biases generated with ANN

$W_{i(1,1)}$	$W_{i(1,2)}$	$W_{i(1,3)}$	$W_{i(1,4)}$	$W_{i(1,5)}$	$W_{i(1,6)}$	$W_{i(1,7)}$	$W_{i(1,8)}$	$W_{i(1,9)}$
-1.7835	-0.5471	5.7316	0.1280	-3.3333	-.4.4575	0.5641	5.5534	0.7681
$W_{i(2,1)}$	$W_{i(2,2)}$	$W_{i(2,3)}$	$W_{i(2,4)}$	$W_{i(2,5)}$	$W_{i(2,6)}$	$W_{i(2,7)}$	$W_{i(2,8)}$	$W_{i(2,9)}$
0.4583	0.1204	3.0152	0.0034	-5.5121	-2.8901	0.4422	3.0987	0.6342
$W_{i(3,1)}$	$W_{i(3,2)}$	$W_{i(3,3)}$	$W_{i(3,4)}$	$W_{i(3,5)}$	$W_{i(3,6)}$	$W_{i(3,7)}$	$W_{i(3,8)}$	$W_{i(3,9)}$
0.2376	1.2708	-0.9067	0.0043	-0.4163	-1.1023	0.3312	4.0456	0.4879
$W_{o(1,1)}$	$W_{o(1,2)}$	$W_{o(1,3)}$	$W_{o(1,4)}$	$W_o(1,5)$	$W_{o(1,6)}$	$W_{o(1,7)}$	$W_{o(1,8)}$	
0.0678	-0.6929	-0.1069	-0.7079	-0.9213	0.1101	-0.1192	0.0721	
$B_{1(1)}$	$B_{1(2)}$	$B_{1(3)}$	$B_{1(4)}$	$B_{1(5)}$	$B_{1(6)}$	$B_{1(7)}$	$B_{1(8)}$	
0.4407	-3.3456	0.5181	6.6727	0.3321	-3.9234	0.5002	4.1230	
$B_{2(1)}$								
-0.3456								
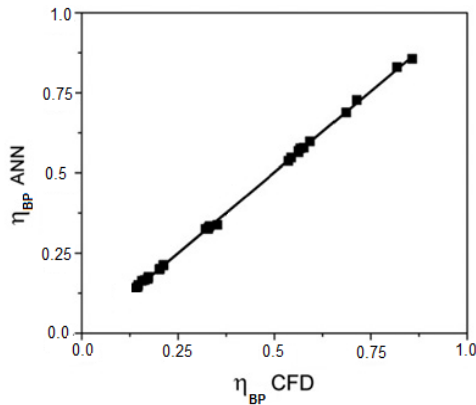
Fig. 12. Comparison of ANN and CFD based base pressure results.

implied that the ANN model anticipated base pressure with least deviation when contrasted with the one anticipated by CFD. The values predicted by ANN have been in good agreement with the CFD values. Table 3 presents the ANN weights, biases and coefficients. The Fig. 13 shows the plot for comparison of ANN and CFD predicted base pressure values for 18 data sets/training patterns. The maximum error observed was 10%. Post training, 6 patterns were used for testing purpose. Figure 14 shows the plot for ANN and CFD predicted base pressure values for 6 testing data set. It was observed that the ANN and CFD predicted base pressure values are close to each other with an RMSE=0.0045. For the testing data sets, the absolute error was found to be below 5%. The prediction of base pressure discovers its applications like ignition chamber where the base pressure is to be kept up at the very least dimension so as to boost mixing. Additionally on account of rockets and projectiles, the base pressure ought to be kept up to a most extreme to limit the base drag. The anticipated outcomes will assist the aerodynamic engineers to specify precise values while structuring aerodynamic vehicles.

4.3 Relative Importance of input Variables

The general significance of the input factors was resolved utilizing the condition proposed by Garson (1991) and that relative significance is concerned with ANN associated weights at ANN layers. In Fig.

15, the outcomes demonstrate that the Mach number is the most significant parameter with a 47.16% of relative significance, trailed by NPR (28.35%), and area ratio (24.47%).

4.4 Interaction of Input Variables

The ANN mathematical model derived has been employed to identify the relationship between the input parameters and base pressure. In Fig. 16, three contours of pressure are shown as function of M, NPR and AR. From Fig. 16(a) it was seen that an expansion in Mach number will build the base pressure steadily and concurrently, an expansion in NPR diminishes the base pressure. This is fundamentally because of the high over development of the planes at Mach 2.5 and 3.0 that confronts a shock at the nozzle/duct interface in this manner demonstrating a solid direct relationship of Mach number with base pressure. Smaller deflections and greater angles are retained by these shocks. As a matter of fact even though these shocks tend to cause a definitive increment in the base pressure, they will attain a particular position, and as a result do not effect base region much. Thus recirculation flow monopolizes over shock flow (Khan and Rathakrishnan 2002, 2003, 2004a). It is likewise watched that contribution of Mach number towards this response is more looked at to that of NPR. The Fig. 16(b) outlines the impact of Mach number and area proportion on base pressure. As the area ratio increases, the base pressure also expands. This conduct of increase in base pressure values is due to the fact that the flow relishes the relaxation and also that, not enough creation of suction by the vortex which contrarily does so for low area ratios (Khan and Rathakrishnan, 2004b and Quadros *et al.*, 2017). Figure 16(c) demonstrates decline in base pressure for expanded dimensions of NPR. A more critical take on the base region will give a conceivable interpretation to this case. For a given area ratio, the level of development that takes place at the nozzle exit decides the base pressure level. The prime interest is the dimension of over development. This over extension develops a shock at the nozzle exit for lower NPRs, bringing about an exceptionally abnormal state of base pressure (Khizar *et al.,* 2018). This shock turns fragile as the level of over development diminishes (Khan and Rathakrishnan,
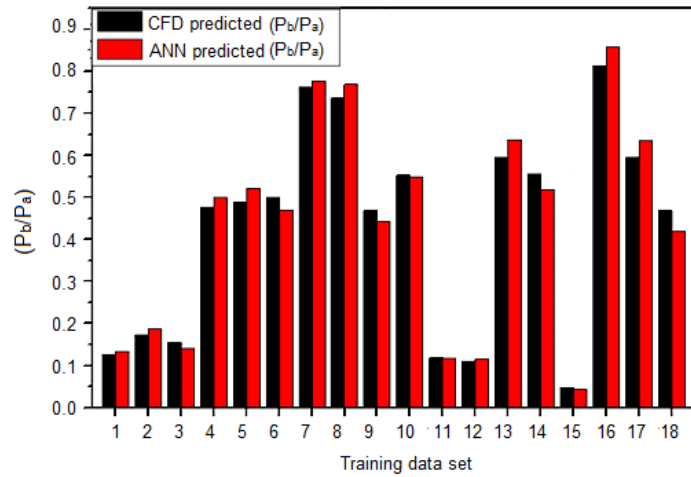
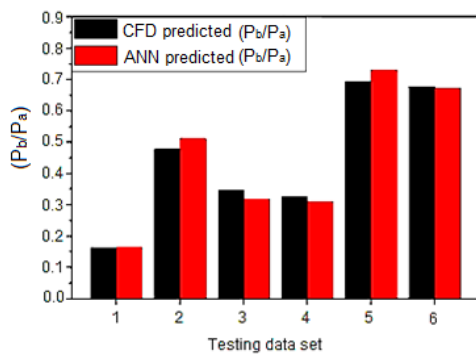**Fig. 13. Comparison of training data set for base pressure predicted by ANN and CFD.**

Fig. 14. Comparison of testing data set for base pressure predicted by ANN and CFD.
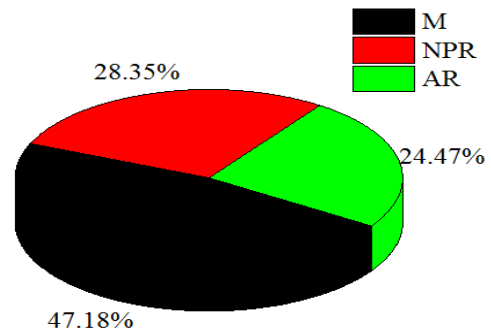

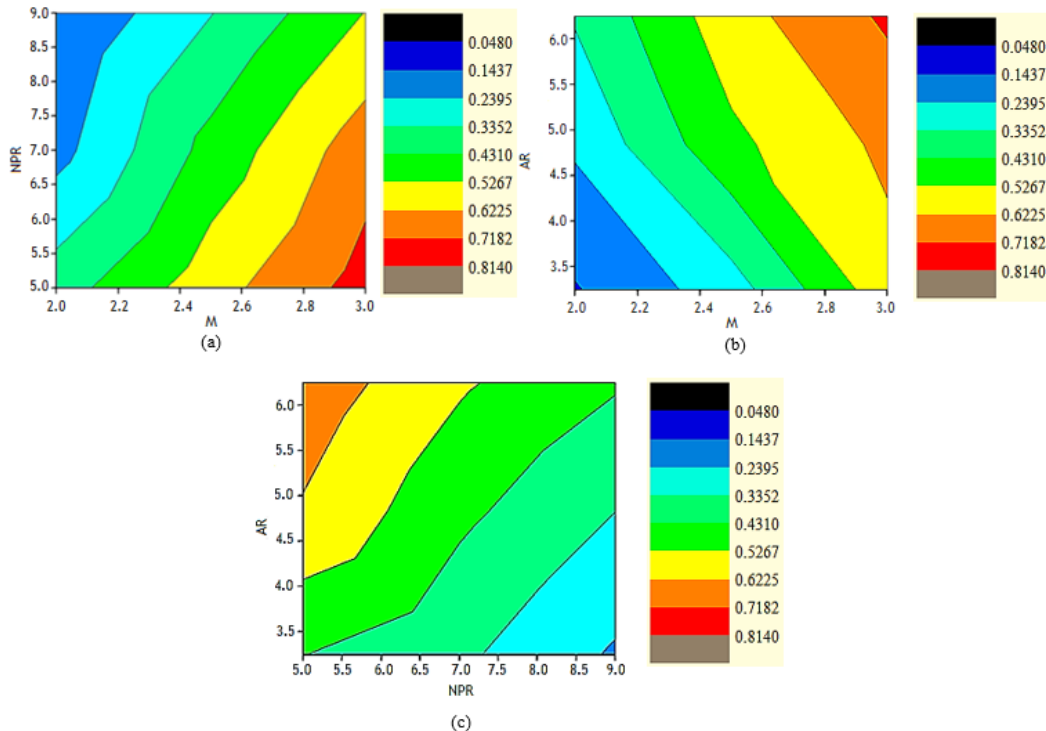**Fig. 15. Relative importance of the input variables.**

Fig. 16. Surface plots of non-dimensional base pressure with (a) Mach number and NPR, (b) Mach number and AR, (c) NPR and AR.

2003, 2004b). It is additionally seen that commitment of area ratio towards this response is high (because of its precarious increment) when contrasted with that of NPR. Henceforth the variety of base pressure concerning NPR is by all accounts linear, though area ratio implies to be marginally nonlinear.

5. CONCLUSION

The flow process developed in a suddenly expanded duct has been predicted by use of CFD and ANN methodology. M, NPR and AR were the parameters considered for the study. The CFD and ANN results have been in good agreement with each other with a correlation co-efficient of $R^2 > 0.99$ and a RMSE = 0.0032. The anticipated dependability of the model was demonstrated with tests excluded in the database, and its performance was successful with a RMSE = 0.0045. It is in this way presumed that, the created ANN model can be utilized to forecast base pressure successfully without turning to costly computational simulations. Sensitivity analysis revealed that Mach number (M) is the most consequential parameter that affected base pressure in the current study. This was followed by NPR and AR. The ANN model was then adopted to identify the relationship between input parameters. It was observed that a combination of higher Mach number and high area ratio yielded a higher base pressure. On the contrary, an increase in NPR developed low base pressure values. Therefore the above model obtained could be used for optimization of base pressure for various applications viz. rockets, missiles and combustion chambers.

EFERENCES

Alvi, F. S., C. Shih, R. Elavarasan, G. Garg and A. Krothapalli (2003). Control of supersonic impinging jet flows using supersonic microjet. *American Institute of Aeronautics and Astronautics Journal* 41, 1347-1355.

Baig, M. A. A., F. S. Al-Mufadi, S. A. Khan and E. Rathakrishnan (2011). Control of Base Flows with Micro jets. *International Journal of Turbo and Jet Engines* 28, 259-269.

Bansal R. and R. B. Sharma (2014). Drag Reduction of Passenger Car Using Add-On Devices. *Journal of Aerodynamics* 1-13.

Baymani, M., S. Effati, H. Niazmand and A. Kerayechian (2015). Artificial neural network method for solving the Navier-Stokes equations. *Neural Computing & Applications* 26, 765-773.

Farahani, M. and A. Jaberi (2017). Experimental Investigation of Shock Waves Formation and Development Process in Transonic Flow. *Scientia Iranica B*, 24, 2457-2465.

Fontama, V. N., K. Jambunathan, S. L. Hartle and F. S. Ashforth (1997). Using ART2 networks to deduce flow velocities. *Artificial Intelligence in Engineering* 11, 135-141.

G. D. Garson (1991). Interpreting neural-network connection weights. *AI Expert* 6, 47–51.

Gholami, A., H. Bonakdari, A. H. Zaji and A. A. Akhtari (2015). Simulation of open channel bend characteristics using computational fluid dynamics and artificial neural networks. *Engineering Applications of Computational Fluid Mechanics* 9, 355-369.

Gregory, J. Z., M. C. Louay and D.W. Keith (2007). Heat transfer and friction in helically finned tubes using artificial neural networks. *International Journal of Heat and Mass Transfer* 50, 4713-4723.

Karthick, S. K., M. V. Rao, G. Jagadeesh and K. P. J. Reddy (2018). Experimental parametric studies on the performance and mixing characteristics of a low area ratio rectangular supersonic gaseous ejector by varying the secondary flow rate. *Energy* 161(15), 832-845

Khan, S. A. and E. Rathakrishnan (2002). Active Control of Suddenly Expanded Flows from Over expanded Nozzles. *International Journal of Turbo and Jet Engine* 19, 119-126.

Khan, S. A. and E. Rathakrishnan (2003). Control of Suddenly Expanded Flows with Micro Jets. *International Journal of Turbo and Jet Engines* 20, 63-81.

Khan, S. A. and E. Rathakrishnan (2004a). Active Control of Suddenly Expanded Flow from Under Expanded Nozzles. *International Journal of Turbo and Jet Engines* 21, 233-253.

Khan, S. A. and E. Rathakrishnan (2004b). Control of Suddenly Expanded Flow from Correctly Expanded Nozzles. *International Journal of Turbo and Jet Engines* 21, 255-278.

Khan, S. A. and E. Rathakrishnan (2006). Control of Suddenly Expanded Flow. *Aircraft Engineering and Aerospace Technology: An International Journal* 78, 293-309.

Khizar, A. P., P. S. Dabeer and S. A. Khan (2018). Optimization of area ratio and thrust in suddenly expanded flow at supersonic Mach numbers. *Case studies in Thermal Engineering* 12, 696-700.

Korst, H. (1956). A Theory of base pressure in Transonic and Supersonic flow. *Journal of applied Mechanics* 23, 593-600.

Launder, B. E. and D. B. Spalding (1972). *Lectures in mathematical models of turbulence*. Academic Press, London, 1972.

Montazer, E., H. Yarmand, E. Salami, M. R. Muhamad, S. N. Kazi and A. Badarudin (2018). A brief review study of flow phenomena over a backward-facing step and its optimization. *Renewable and Sustainable Energy Reviews* 82, 994-1005.

Quadros, J. D., S. A. Khan and A. J. Antony (2017). Study of Effect of flow parameters on base pressure in a suddenly expanded duct at

supersonic Mach number regimes using CFD and design of experiments. *Journal of Applied Fluid Mechanics* 11, 483-496.

Quadros, J. D., S. A. Khan and A. J. Antony (2018). Modelling of suddenly expanded flow process in supersonic Mach regime using design of experiments and response surface methodology. *Journal of Computational Applied Mechanics* 49, 149-160.

Quadros, J. D., S. A. Khan, A. J. Antony and J. S. Vas (2016). Experimental and numerical studies on flow from axisymmetric nozzle flow with sudden expansion for Mach 3.0 using CFD. *International Journal of Energy, Environment,* *and Economics* 24, 87-97.

Rathakrishnan, E. and A. K. Sreekanth (1984). Flow in pipes with sudden enlargement. *Proceedings of the 14th International Symposium on Space Technology and Science*, Tokyo, Japan.

Tu, J., G. Y. Heng and C. Liu (2007). Computational fluid dynamics—A practical approach. Elsevier Science & Technology, New York, USA.

Wilcox J .F. Jr. (1988). Passive venting system for modifying cavity flow fields at supersonic speeds. *AIAA Journal* 26, 374-376.